Biochimica et Biophysica Acta, 352 (1974) 412–440

BBA 76650

MASS TRANSFER OF CO_2 ACROSS MEMBRANES: FACILITATION IN THE PRESENCE OF BICARBONATE ION AND THE ENZYME CARBONIC ANHYDRASE

SHYAM R. SUCHDEO and JEROME S. SCHULTZ

Department of Chemical Engineering, The University of Michigan, Ann Arbor, Mich. 48104 (U.S.A.)

(Received September 21st, 1973)

SUMMARY

A theoretical and experimental analysis of facilitated transport of CO_2 across membranes containing $NaHCO_3$ and the enzyme carbonic anhydrase (carbonate hydro-lyase EC 4.2.1.1) is presented. The necessary diffusion reaction equations are derived and the system constraints defined. For the CO_2–HCO_3^- system, mathematical simplifications based on the magnitude of various reaction and concentration terms are made to make the equations tractable to solution. The resultant equations are solved by a number of analytical and numerical techniques, each having a limited, though useful, range of validity.

The experimental arrangement consists of a liquid membrane (created by soaking a porous filter paper in the test solution), a diffusion chamber, and gas metering and analysis equipment. Conditions were selected to cover the range from diffusion- to reaction-dominated behavior.

The flux of CO_2 across a membrane containing 1 M $NaHCO_3$ was measured at various partial pressures of CO_2 (2–28 in Hg) and with membrane thicknesses of 0.02, 0.06 and 0.10 cm. The extent of facilitation (defined as the ratio of reaction-related flux to the expected Fick's Law flux in the absence of reaction) ranged from near zero to nearly 5 in these experiments. The agreement between model calculations and experimental observation was found to be excellent over the entire range of near-diffusion to near-equilibrium behavior.

In the presence of enzyme carbonic anhydrase (0.10 mg/ml, activity approx. 80%) and 1 M $NaHCO_3$, the CO_2 flux across a 0.02 cm membrane was 3–10-fold higher than the corresponding flux in the absence of enzyme. From experiments at various enzyme concentrations and membrane thicknesses, it appeared that the apparent CO_2 reaction rate was directly proportional to the enzyme concentration. The model calculations for the enzyme-catalyzed reactions agreed with the experimental observations to within $\pm 10\%$.

INTRODUCTION

Facilitated transport process reported in this work refers to the transfer of permeant(s) across a liquid film containing "entrapped" chemical species with which

the dissolved permeant(s) react in solution. By definition, the flux of the "entrapped" species, also referred to as the non-transferred or carrier species, is zero at the two physical boundaries; this in contrast to other facilitated transport studies where some or all the components may enter or leave the membrane phase [1]. In addition, the physical dimensions of the liquid film (that is, thickness and transfer area) are assumed known and only homogeneous reactions take place in the solution. The theoretical treatment of facilitated transport phenomenon, also referred to as "carrier-mediated" transport, has been based on a model allowing for concurrent processes of diffusion and reversible chemical reaction.

This report concerns itself with the facilitated transport of CO_2 across strongly basic aqueous films. Early experiments by Ward [2] had indicated that across an aqueous film containing a weak base, such as pyridine, the observed flux of CO_2 increased to a level twice that across a corresponding water film. In the presence of a strong base, such as saturated $CsHCO_3$ solution, Ward and Robb [3] observed that the relative flux ratio of CO_2 to O_2 increased by a factor of 75. Experiments by Longmuir et al. [4] and by Ward and Robb [3] indicated that the CO_2 flux could also be increased by catalyzing the CO_2 reactions; among the catalysts used for this purpose were sodium aresenite and enzyme carbonic anhydrase. Later experiments by Enns [5] demonstrated that CO_2 flux across buffer solutions was enhanced by orders of magnitude in the presence of enzyme carbonic anhydrase. More recently, Otto and Quinn [6] investigated the CO_2–HCO_3^- system in further detail. In their experiments, the CO_2 partial pressures at the two gas–liquid interfaces were always maintained at 1 and 0 atm, and the observed CO_2 facilitation in the absence of the enzyme was rather small. In the presence of varying amounts of carbonic anhydrase, Otto and Quinn indicate an apparent abnormality in the enzymatic reactions. Based on a calculated equilibrium flux of CO_2, the ratio of observed CO_2 flux to the equilibrium CO_2 flux went through a maxima at an enzyme concentration of approximately 0.5 mg/ml.

The above investigations were limited in their scope – experimental as well as theoretical. Here, the $CO_2 - HCO_3^-$ facilitation process is studied in further detail to encompass a larger range of experimental variables, and to present a more general theoretical analysis. The principal features of the CO_2 facilitation process are as follows: (a) in the uncatalyzed reaction scheme, a total of nine chemical species participate in six reactions, (b) only the CO_2 reactions are rate limiting, (c) a variable reaction "rate constant" which can be obtained by varying amount of carbonic anhydrase concentration in the film, and (d) transport, solubility, and kinetic constants change as the HCO_3^-–CO_3^{2-} concentration is increased.

The mathematical equations governing the transport process are, in general, highly non-linear. To this must be added the complexity arising from the zero-flux condition on the carrier species. The theoretical objective was therefore to obtain a unified overall picture of the phenomenon based on various limiting analytical as well as approximate solutions. Such solutions have been reported in the literature for specific examples; a principal task was therefore to generalize the approach so as to accommodate the overall phenomenon. In addition, the CO_2 facilitation system required that a method for handling multiple reactions be obtained. The regimes in which the analytical and approximate solutions are valid may be defined as (a) near-diffusion regime [7], (b) near-equilibrium regime [8], (c) boundary-layer approximation [9, 10], (d) near-stationary state regime [11], (e) large carrier concentration limit [2].

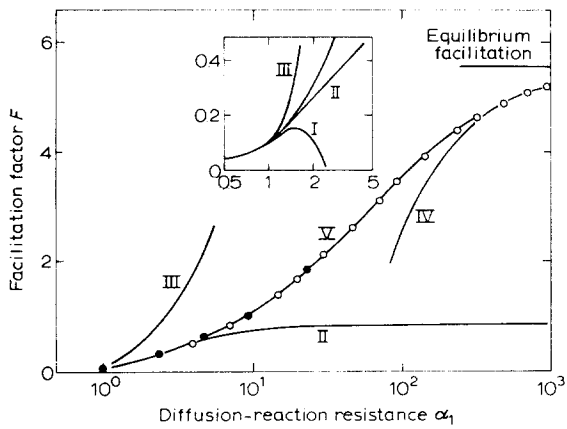

Fig. 1. Calculated facilitations in the flux of CO_2 as a function of Damköhler number α_1. Curves I through IV are limiting analytical solutions. Curve V represents numerical solution by quasilinearization (●—●) and boundary layer approximation solution (○—○). Model approximations: I, near-diffusion; II, near-stationary state; III, large carrier; IV, near-equilibrium; V, "exact".

TABLE I

PHYSICOCHEMICAL CONSTANTS AT 25 °C

	In water		In 1 M $NaHCO_3$–Na_2CO_3 solution	
k_1, s^{-1}	0.0375	[17]		
	0.0358	[18]		
	0.026	[19]		
K_1	$2.58 \cdot 10^{-3}$	[20]		
k_2, $cm^3 \cdot gmole^{-1} \cdot s^{-1}$	$8.5 \cdot 10^6$	[19]		
K_1K_3, gmoles/cm^3	$4.56 \cdot 10^{-10}$	[20]	$1.37 \cdot 10^{-9}$	[16]
K_4, gmoles/cm^3	$4.69 \cdot 10^{-14}$	[20]	$2.70 \cdot 10^{-13}$	[21]
K_6, (gmoles/cm^3)^2	$1.01 \cdot 10^{-20}$	[20]	$1.56 \cdot 10^{-20}$	[21]
K', gmoles $\cdot$ $cm^{-3} \cdot atm^{-1}$	0.33		0.105	[22]
n	24.4		11.46	[23]
k_p, s^{-1}	$8 \cdot 10^5$	[13]★		
K_{ms}, gmoles/cm^3	$1.2 \cdot 10^{-5}$	[13]★		
K_H, gmoles/cm^3	$4.6 \cdot 10^{-13}$	[13]★		
D_1, cm^2/s	$1.96 \cdot 10^{-5}$	[14]		
H_1, gmoles $\cdot$ $cm^{-3} \cdot atm^{-1}$	$3.39 \cdot 10^{-5}$	[15]		
D_1H_1, gmoles $\cdot$ $cm^{-1} \cdot atm^{-1} \cdot s^{-1}$			$3.80 \cdot 10^{-10}$	[7]
D_2, D_3, cm^2/s	$1.08 \cdot 10^5$★★		$0.89 \cdot 10^{-5}$★★	

★ Carbonic anhydrase isolated from bovine red blood cells.
★★ See text: Physiochemical parameters.

Several factors dictate the validity of each approximation; the principal parameter being the Damköhler number, defined as the ratio of diffusion to reaction resistance. Fig. 1 is an example of the extent of facilitation as a function of Damköhler number. Various limiting solutions as well as the numerical solution are indicated. A detailed discussion is presented in a later section.

The experimental objective of this study was to investigate the CO_2 facilitation over a wide range of variables. In the near-diffusion regime, information pertaining to diffusivity and solubility of gases in reacting solutions was obtained [7]. In the near-equilibrium regime, the relative importance of parameters such as CO_2 partial pressures at the two interfaces and carbonic anhydrase concentration is investigated, The experimental variables covered in this study are: Total HCO_3^- concentration, 1 gmole/l; diffusion path length, 0.02–0.10 cm; CO_2 partial pressure, 0.001–1 atm; enzyme concentration, 0.1–1 mg/ml.

NOMENCLATURE

A_i	Chemical species i
C_i	Dimensionless concentration of A_i,
C_i^0	Dimensionless total concentration of A_i,
$\hat{C}_i$	Concentration of A_i, gmoles/cm^3
$\hat{C}_i(0)$, $\hat{C}_i(L)$	$\hat{C}_i$ at $y = 0, L$, respectively, gmoles/cm^3
$\hat{C}_i^0$	Total concentration of A_i, gmoles/cm^3
$\bar{C}_i$, $\bar{C}_i$	Dimensionless concentration of A_i at $x = 0$, 1, respectively
$\bar{C}_1$	Dimensionless CO_2 concentration defined in Eqn 26
D_i	Diffusivity of A_i in the reaction solution, cm^2/s
D_i^0	Diffusivity of A_i in the solvent, cm^2/s
E_0	Total enzyme concentration, gmoles/cm^3
F	Facilitation factor defined in Eqn 18
F^e	Equilibrium facilitation factor
f	Activity coefficient
g_{ij}	Diffusion-stoichiometric ratio of A_i defined in Eqn 15
H_1, H_1^0	Henry's Law constant, gmoles $\cdot$ cm^{-3} $\cdot$ atm^{-1}
I_i	Reaction invariant defined in Eqn 11
K	Overall equilibrium constant defined in Eqn 21
K_i	Equilibrium constant for ith reactions
K_H, K_{ms}, K_{mi}	Equilibrium constants for enzyme-catalyzed reactions, gmoles/cm^3
k_i	Forward rate constant for ith reaction
k_p	Rate constants for enzyme catalyzed reaction, s^{-1}
L	Diffusion path length, cm
m	Equilibrium constant defined in Eqn 26
N_i	Flux of A_i, gmoles $\cdot$ cm^{-2} $\cdot$ s^{-1}
N_1^0	Fick's Law flux of A_i through the reaction solution, gmoles $\cdot$ cm^{-2} $\cdot$ s^{-1}
N_1^e	Equilibrium flux of A_1, gmoles $\cdot$ cm^{-2} $\cdot$ s^{-1}
N_1^w	Fick's Law flux of A_1 through solvent, gmoles $\cdot$ cm^{-2} $\cdot$ s^{-1}
n	Rate constant defined in Eqn 26
P_0, P_L	Partial pressure of A_1 at $y = 0, L$, respectively, atm

Q	Enzyme mechanism defined in Eqn 27
r_i	Rate of consumption of A_i, gmoles $\cdot$ cm$^{-3} \cdot$ s^{-1}
u_i	Ionic mobility
V_1, $V_1{}^0$	CO_2 flux, cm^3/min
x	Dimensionless distance
y	Distance into the film, $0 \leqq y \leqq L$, cm

Greek symbols

α_i	Diffusion-reaction parameter defined in Eqn 15
ε_1	$= 1/\alpha_1$
η	Constant defined in Eqn 30
η'	Relative solution viscosity
μ^i	Electrophoretic effect term, cm^2/s
ν_{ij}	Stoichiometric coefficient of A_i in jth reaction
ξ_{ij}	Coefficient of reaction invariant defined in Eqn 11
ρ	Dimensionless downstream CO_2 concentration defined in Eqn 15
Φ_i	Dimensionless equilibrium reaction rate
ϕ_i	Dimensionless kinetic functions defined in Eqn 15
ϕ^j	$\partial\phi/\partial C_j$
ϕ^{jk}	$(1/2)\partial^2\phi/\partial C_j \partial C_k$
ω_i	Rate of reaction (forward) of ith reaction, gmoles $\cdot$ cm$^{-3} \cdot$ s^{-1}
Overbars	Denote evaluation at or near $x = 0$
Underbars	Denote evaluation at or near $x = 1$
Superscript	jth perturbation

CO_2 FACILITATION MODEL

Before proceeding to derive the necessary equations for the CO_2 facilitation model, we will consider the chemistry and kinetics of the reactions. Dissolution of CO_2 in water is accompanied by the formation of the hydrated compound, H_2CO_3, which subsequently dissociates into HCO_3^-, CO_3^{2-}, and H^+ (see Kern [12] for historical background). The first step in the neutralization reaction involves the reaction of dissolved CO_2 by either one or both of the following mechanisms:

$$\text{(i)}\quad CO_2 + H_2O \underset{k_{-1}}{\overset{k_1}{\rightleftarrows}} H_2CO_3 \qquad (\text{pH} \leqq 8)$$

$$\text{(ii)}\quad CO_2 + OH^- \underset{k_{-2}}{\overset{k_2}{\rightleftarrows}} HCO_3^- \qquad (\text{pH} \geqq 10) \tag{1}$$

Whereas Reactions i and ii, Eqn 1, have finite rate constants, the following extremely rapid reactions are also involved in the reaction scheme:

$$\text{(iii)}\quad H_2CO_3 \rightleftarrows H^+ + HCO_3^-;\ K_3$$
$$\text{(iv)}\quad HCO_3^- \rightleftarrows H^+ + CO_3^{2-};\ K_4 \tag{2}$$

In the study of the facilitated transport of CO_2, the reactions listed in Eqns 1 and 2 are carried out in the presence of a base, for example $NaHCO_3$, and the following rapid and complete dissociation reaction is also to be expected:

$$\text{(v)}\quad MHCO_3 \rightleftarrows M^+ + HCO_3^-;\ K_5 \cong \infty \tag{3a}$$

To the above set of reactions must be added yet another for the rapid dissociation of water:

$$\text{(vi)}\quad H_2O \rightleftarrows H^+ + OH^-;\ K_6 \tag{3b}$$

The overall reaction between CO_2, HCO_3^-, and CO_3^{--} may be written as

$$CO_2 + CO_3^{2-} + H_2O \rightleftarrows 2HCO_3^- \tag{4}$$

Since reaction mechanisms i and ii, Eqn 1, are the limiting steps in the overall scheme of reactions, carbonic anhydrase, a catalyst for these steps was used to study the effect of an enhanced rate of reaction on facilitation. Indications are that the enzyme-catalyzed hydration and dehydration reaction obeys the following mechanism [13]:

$$CO_2 + H_2O + E \overset{K_{ms}}{\rightleftarrows} X \underset{k_p'}{\overset{k_p}{\rightleftarrows}} HCO_3^- + H^+ + E \tag{5}$$

where E is the enzyme carbonic anhydrase (E^-, EH)
and X is an intermediate of the reaction (ECO_2^-, $EHCO_2$)

The hydration and the inhibition reactions of the enzyme are

$$E^- + H^+ \overset{K_H}{\rightleftarrows} EH \tag{6}$$
$$E + HCO_3^- \overset{K_{mi}}{\rightleftarrows} EHCO_3^- (E = E^-, EH)$$

Physicochemical parameters

In order to calculate the flux of CO_2, several parameters must be known or evaluated. These are the rate and equilibrium constants (for the uncatalyzed as well as the enzyme-catalyzed reactions), diffusivities, and the solubility of CO_2 in the reactant solution.

Values for the various rate and equilibrium constants given in the literature are summarized in Table I. The salts $MHCO_3$, M_2CO_3 are assumed to be completely dissociated. The value of K_{mi} remains unknown at this time.

The widely accepted values quoted in the literature for the diffusivity D_1 and the solubility H_1 of CO_2 in water are $1.96 \cdot 10^{-5}$ cm^2/s [14] and $3.39 \cdot 10^{-5}$ gmoles $\cdot$ cm$^{-3} \cdot$ atm^{-1} [15], respectively. In this study, however, it was necessary to know the effect of concentration and ionic strength on these parameters, since $NaHCO_3$–Na_2CO_3 solutions were used in the facilitation experiments. In a related publication, we estimated the physical permeability (D_1H_1) of CO_2 through HCO_3^- solutions (1 M) to be $3.80 \cdot 10^{-10}$ gmoles $\cdot$ cm$^{-1} \cdot$ atm$^{-1} \cdot$ s^{-1} [7].

The ionic diffusivities of HCO_3^- and CO_3^{2-} depend on the individual ionic mobilities as well as their concentrations. In dilute solutions, the diffusivities are bounded by the following two limits:

$$D_2^0, D_3^0 \leqq (RTu_2/2, RTu_3)$$

and, at 25 °C, the limits are [16]:

$$\frac{RTu_2}{2} = 0.92 \cdot 10^{-5} \text{ cm}^2/\text{s}$$

$$RTu_3 = 1.18 \cdot 10^{-5} \text{ cm}^2/\text{s}$$

(Subscripts 2 and 3 refer to CO_3^{2-} and HCO_3^-, respectively.)

In light of the fact that the two bounds for D_2^0 and D_3^0 are nearly the same, we assumed that the diffusivities of HCO_3^- and CO_3^{2-} are equal and a common value was selected arbitrarily at a HCO_3^- concentration equal to twice the CO_3^{2-} concentration; thus $D_2^0 \cong D_3^0 \cong 1.08 \cdot 10^{-5}$ cm^2/s.

In concentrated solutions, ionic diffusivities D_i can be obtained from [16]

$$D_i = (D_i^0 + \mu^i)\left(1 + \frac{\text{dln}f}{\text{dln}\hat{C}}\right)\eta' \tag{20}$$

For a 1 M $NaHCO_3$–Na_2CO_3 solution, the 'correction' terms for the HCO_3^- and CO_3^{2-} are estimated as

$$\mu^i \approx 0.04 \cdot 10^{-5} \text{ cm}^2/\text{s} \tag{7}$$

$$\frac{\text{dln}f}{\text{dln}\hat{C}} \approx -0.007$$

and the relative solution viscosity is taken as the average of $NaHCO_3$ and Na_2CO_3 solution viscosities [24]: $\eta' = 1.27$. Therefore, for a one normal solution, the ionic diffusivities of the HCO_3^- and the CO_3^{2-} are estimated to be $D_2 \approx D_3 \approx 0.89 \cdot 10^{-5}$ cm^2/s.

Model formulation

In presenting the equations for the facilitation of CO_2, the derivation for the uncatalyzed reaction scheme, Eqns 1–3, is shown in detail. A model for the enzymatically catalyzed reaction scheme may be similarly derived. The development is based on the premise of diffusion accompanied by homogeneous reversible chemical reaction everywhere within the film. Sufficient boundary conditions for the diffusion–reaction equations are obtained from a knowledge of concentrations (or partial pressures) of the transferred species at the gas–liquid interfaces and the zero-flux condition on entrapped species.

We will adopt the following notation to simplify the presentation of the various diffusion–reaction equations. The various chemical species are denoted as follows:

Subscript i	Species A_i
1	CO_2
2	CO_3^{2-}
3	HCO_3^-
4	M^+
5	H^+
6	$MHCO_3$
7	OH^-
8	H_2O
9	H_2CO_3

The overall reaction, Eqn 4, is represented as

$$-A_1 - A_2 - A_8 + 2A_3 = 0 \tag{8}$$

and the six individual mechanistic steps, Eqns 1–3, are given in matrix form by

$$[\nu]^T(A) = (0) \tag{9}$$

where ν_{ij} component of the matrix $[\nu]$ represents the stoichiometric coefficient of i^{th} species participating in the j^{th} reaction:

$$[\nu] \equiv \begin{pmatrix} -1 & -1 & 0 & 0 & 0 & 0 \\ 0 & 0 & 0 & 1 & 0 & 0 \\ 0 & 1 & 1 & -1 & 1 & 0 \\ 0 & 0 & 0 & 0 & 1 & 0 \\ 0 & 0 & 1 & 1 & 0 & 1 \\ 0 & 0 & 0 & 0 & -1 & 0 \\ 0 & -1 & 0 & 0 & 0 & 1 \\ -1 & 0 & 0 & 0 & 0 & -1 \\ 1 & 0 & -1 & 0 & 0 & 0 \end{pmatrix}$$

A cursory examination of the stoichiometric coefficients $[\nu]$ and column operations reveals that only five of the mechanistic steps are stoichiometrically independent. For convenience, the first five reaction rates are chosen to be the linearly independent set. That is, $\nu_{i6} = \nu_{i1} - \nu_{i2} + \nu_{i3}$.

Denoting ω_j as the net rate (forward) of reaction j, the rate of consumption of A_i is given by

$$-(r) = [\nu](\omega) \tag{10}$$

Now, by row operations on the matrix $[\nu]$, one finds that certain combinations of reaction rates for various species cancel each other out. The reaction rates of A_6 through A_9 are then given by the following linear equations:

$$\begin{aligned} r_6 &= -r_4 \\ r_7 &= -2r_2 - r_3 + r_4 + r_5 \\ 2r_8 &= -r_3 - r_5 - r_6 - r_7 + 2r_9 \\ r_9 &= -r_1 - r_2 - r_3 - r_6 \end{aligned}$$

These relations determine some invariant properties of the system, which in this case are four in number

$$I_k \equiv \sum_{i=1}^{9} \xi_{ki} r_i = 0, k = 1, 4, \text{ or} \tag{11}$$

$$r_4 + r_6 = 0$$

$$2r_2 + r_3 - r_4 - r_5 + r_7 = 0$$

$$r_3 + r_5 + r_6 + r_7 + 2r_8 + 2r_9 = 0$$

and

$$r_1 + r_2 + r_3 + r_6 + r_9 = 0$$

Of these four relationships, first three are seen to be independent of r_1, the reaction rate of the transferred species.

Up to this point, we have only considered stoichiometric relationships which result from the kinetic steps in the CO_2 reaction mechanism. To complete the analysis one must consider the diffusion process; in general the unsteady-state conservation diffusion equations for each of the species involved are of the form

$$\frac{\partial \hat{C}_i}{\partial t} = \frac{\partial N_i}{\partial y} + r_i, \qquad i = 1, 9 \tag{12}$$

Of these, the first five form, once again, a linearly independent set. For $i = 6, 8$, a set of three integral relationships is obtained corresponding to a subset of the reaction invariants given in Eqn 11, i.e. those not involving the permeable species, CO_2 [25] or

$$1/L \int_0^L \sum_{i=2}^{9} \xi_{ki} \hat{C}_i \, dy = \hat{C}_k^0, \text{ or} \tag{13}$$

$$1/L \int_0^L (\hat{C}_4 + \hat{C}_6) dy = \hat{C}_6^0$$

$$1/L \int_0^L (2\hat{C}_2 + \hat{C}_3 + \hat{C}_7 - \hat{C}_4 - \hat{C}_5) dy = 0$$

and

$$1/L \int_0^L (\hat{C}_3 + \hat{C}_5 + \hat{C}_6 + \hat{C}_7 + 2\hat{C}_8 + 2\hat{C}_9) dy = 2\hat{C}_8^0$$

On inspection, the three integral constraints are seen to define the time invariant "species" of the system, namely, total metal M, total charge density, and total hydrogen H.

Defining the flux N_i for any species (ionic or molecular) via a binary diffusivity, that is, neglecting any diffusive coupling effect,

$$N_i = -D_i \frac{d\hat{C}_i}{dy}$$

and, further treating the diffusivity as being independent of concentration (dilute solution), Eqn 12 under steady state becomes

$$D_i \frac{d^2 \hat{C}_i}{dx^2} = r_i \tag{14}$$

The linearly independent diffusion–reaction equations, Eqn 14, are now dimensionalized to give

$$\frac{d^2 C_i}{dx^2} = \sum_{j=1}^{6} g_{ij} \alpha_j^2 \phi_j, \quad i = 1, 5 \tag{15}$$

where: $g_{ij} = -D_1 \nu_{ij}/D_i$, $\alpha_j^2 = k_j^\star L^2/D_1$, $\phi_j = r_j/(k_j^\star \hat{C}_6{}^0)$, $C_i = \hat{C}_i/\hat{C}_6{}^0$ and $x = y/L$. $k_j^\star$ is a typical first-order rate constant for the j^{th} reaction. The appropriate boundary conditions for Eqn 15 are

$$
\begin{aligned}
&x = 0 \qquad C_1 = \bar{C}_1 \\
&x = 1 \qquad C_1 = \underline{C}_1 \\
&\frac{dC_i}{dx} = 0 \quad \text{at} \quad x = 0, 1, \qquad i = 2, 5
\end{aligned}
\tag{16}
$$

where $\bar{C}_1$ and $\underline{C}_1$ are dimensionless concentrations of C_1 at $x = 0$, 1, respectively. The flux of CO_2 across the film is given by

$$
N_1 = \frac{-D_1 \hat{C}_6^0}{L} \left[\frac{dC_1}{dx}\right]_{x=0} \tag{17}
$$

and the facilitation in the flux of CO_2 is defined as

$$
F = \frac{N_1}{N_1^0} - 1 \tag{18}
$$

At this stage of the development no general analytical solution exists for this set of equations. However, we have established the minimum equations and boundary conditions that are required for a solution. A method for determining which of these are relatively slow and fast reactions to reduce these equations further, as well as the situation of multiple reactions that are rate limiting, is given elsewhere [25].

We are principally interested in solving the CO_2 diffusion–reaction equation, which is

$$
\frac{d^2 C_1}{dx^2} = \alpha_1^2 \phi_1 + \alpha_2^2 \phi_2 \tag{19}
$$

where

$$
\alpha_1^2 = k_1 L^2 / D_1
$$

$$
\alpha_2^2 = k_2 \hat{C}_6^0 L^2 / D_1
$$

and

$$
\phi_1 = C_1 - (1/K_1) C_9
$$

$$
\phi_2 = C_1 C_7 - (1/K_2 \hat{C}_6^0) C_3
$$

Up to this point, the procedure for obtaining the minimal set of equations has been general; to reduce the complexity of the problem further one needs to employ constraints which are particular to a given physical problem. For CO_2 transport, one can use the fact that only Reactions i and ii, Eqn 1, are rate limiting; Eqn 15 may thus be simplified, assuming Reactions iii–vi are at equilibrium everywhere. The equilibrium reactions, Eqns 2 and 3, give:

$$
\begin{aligned}
\Phi_3 &= 0 = C_9 - (\hat{C}_6^0 / K_3) C_3 C_5 \\
\Phi_4 &= 0 = C_3 - (\hat{C}_6^0 / K_4) C_2 C_5 \\
\Phi_6 &= 0 = 1 - (\hat{C}_6^0 / K_6^2) C_5 C_7 \\
\Phi_5 &= 0 = C_6 - (\hat{C}_6^0 / K_5) C_3 C_4
\end{aligned}
\tag{20}
$$

(The water activity coefficient is assumed equal to one.)

Substituting Eqn 20 in Eqn 19 gives

$$\frac{d^2C_1}{dx^2} = \frac{k_1 L^2}{D_1}\left(1+\frac{k_2 K_6}{k_1 K_4}\frac{C_2}{C_3}\right)\left(C_1 - \frac{1}{K}\frac{C_3^2}{C_2}\right) \tag{21}$$

where $K = K_4/K_1K_3$ and $C_1(x=0) = \bar{C}_1$, $C_1(x=1) = \underline{C}_1$.

The integral relationships, Eqn 13, in de-dimensionalized concentrations are

$$\int_0^1 (C_4+C_6)dx = 1 \tag{22}$$

$$\int_0^1 (2C_2+C_3+C_7-C_4-C_5)dx = 0 \tag{23}$$

and

$$\int_0^1 (C_3+C_5+C_6+C_7+2C_8+2C_9)dx = 2C_8^0 \tag{24}$$

The reaction invariance equation, Eqn 11, when substituted into Eqn 14 upon integration gives

$$D_1 C_1 + D_2 C_2 + D_3 C_3 + D_6 C_6 + D_9 C_9 = p'_{13} x + q'_{13} \tag{25}$$

Before proceeding to solve the above set of equations, some further simplifications can be made, again for the CO_2 problem, by consideration of the magnitude for various terms as shown in Appendix I. In light of all these simplifications, the resultant CO_2 diffusion–reaction equations become

$$\frac{d^2\tilde{C}_1}{dx^2} = \alpha_1^2 \phi \tag{26}$$

and

$$\tilde{C}_1 + gC_3 = p_{13}x + q_{13}$$

where

$$\tilde{C}_1 = \hat{C}_1/\hat{C}_1(0)$$

$$\phi = \left(\tilde{C}_1 - m\frac{C_3^2}{1-C_3}\right)\left(1+n\frac{1-C_3}{C_3}\right)$$

$$m = \frac{2\hat{C}_6^0}{(KH_1)P_0} \qquad n = \frac{k_2 k_6}{2k_1 k_4}$$

with $\tilde{C}_1(0) = 1$ and $\tilde{C}_1(1) = \rho$.

The corresponding kinetic function, ϕ_e, and the diffusion reaction resistance, α_e, for the enzyme-catalyzed portion of the total reaction are

$$\phi_e = \left(\tilde{C}_1 - m\frac{C_3^2}{1-C_3}\right)/Q \tag{27}$$

and

$$\alpha_e^2 = \frac{k_p E_0}{K_{ms}} \frac{L^2}{D_1}$$

where Q is either

$$Q_1 = \left(1+\tilde{C}_1 \frac{\hat{C}_1(0)}{K_{ms}}\right)\left(1+C_3 \frac{\hat{C}_6^0}{K_{mi}}\right)\left(1+\frac{C_3}{1-C_3}\frac{2K_4}{K_H}\right)$$

or

$$Q_2 = \left(1+\tilde{C}_1 \frac{\hat{C}_1(0)}{K_{ms}} + C_3 \frac{\hat{C}_6^0}{K_{mi}}\right)\left(1+\frac{C_3}{1-C_3}\frac{2K_4}{K_H}\right)$$

Q_1 refers to the kinetic mechanism proposed by Kernohan [13], discussed earlier in physicochemical parameters. Q_2, on the other hand, refers to a situation wherein the substrate-enzyme binding step has a finite rate (Haldane [26] scheme).

Solution methods

The model equations, Eqn. 26, are now solved to obtain the CO_2 facilitation as a function of several parameters: for example α_1, p_0, p_1, and D_3.

a. Near-diffusion regime. As indicated earlier, various limiting solutions to the model equations, Eqn 26, can be obtained. The solution in the near-diffusion regime, that is, for $\alpha_1 \to 0$, is developed elsewhere [7]. The facilitation in the flux of CO_2 was shown to be given by

$$F = \tfrac{1}{12} Y_0 \alpha_1^2 - \tfrac{1}{720} Y_0 \left[Y_0 - \frac{6-\zeta}{g}\right] \alpha_1^4 + \ldots \tag{28}$$

where

$$Y_0 = 1+n\frac{1-\beta_3}{\beta_3}$$

$$Y_1 = mY_0\left[1-\frac{1}{(1-\beta_3)^2}\right]$$

$$Y_2 = n/\beta_3^2$$

and

$$\zeta = \tfrac{1}{2}(1-\rho)Y_2^2/Y_1^2$$

The constant β_3 is obtained by solving the quadratic equation:

$$m\frac{\beta_3^2}{(1-\beta_3)} = \tfrac{1}{2}(1+\rho) \tag{29}$$

b. Near-equilibrium regime. The limiting analytical solution for $\varepsilon_1 \to 0$ ($\varepsilon_1 = 1/\alpha_1$), based on the development of Goddard et al. [8] and applied to Eqn 26 is

$$\frac{N_1}{N_1^e} = 1 - \varepsilon_1(\bar{\chi} + \underline{\chi}) \tag{30}$$

where

$$\chi = \phi^1 / \eta(\eta^2 - \tilde{\phi}^1)$$

$$\eta^2 = \phi^1 + g\phi^3$$

$$\phi^i = \frac{\partial \phi}{\partial C_i} \quad \text{at} \quad C_i = \psi_i$$

where overbars and underbars refer to evaluation at the boundaries $x = 0, 1$, respectively, and the "equilibrium" bicarbonate concentration ψ_3 is obtained by solving $\Phi \equiv (\phi)_{\psi_i} = 0$ or:

$$m \frac{\psi_3^2}{1 - \psi_3} = \psi_1 \tag{31}$$

with $\psi_1(0) = 1, \psi_1(1) = \rho$.

The convergence of this analytical solution cannot be determined explicitly; the range of α_1 for which Eqn 30 is valid, must therefore be estimated by some alternative method, such as the boundary approximations of Kreuzer and Hoofd [9] and Smith et al. [10].

c. Boundary layer approximation. Based on the generalized equations derived in Appendix II, the boundary layer approximation for the CO_2–HCO_3^- equations, Eqn 26, is as follows:

$$\psi_1(0) = 1 - \frac{\bar{\phi}^1}{\alpha_1 \bar{\eta}^3}(1 - \rho)\frac{N_1}{N_1^0}$$

$$\psi_1(1) = \rho + \frac{\underline{\phi}^1}{\alpha_1 \underline{\eta}^3}(1 - \rho)\frac{N_1}{N_1^0} \tag{32}$$

The solution to Eqn 32 is necessarily iterative. For initiating the iterative procedure, it is assumed that the solution corresponds to the equilibrium chemical reaction limit, that is, $\psi_1(0) \cong 1$ and $\psi_1(1) \cong \rho$.

d. Near-stationary state. The Friedlander–Keller analysis [11] in the near-stationary state, that is, for small (approaching zero) driving force of the transferred species, gives

$$\frac{N_1}{N_1^0} = \frac{1}{1 - \dfrac{Y_0}{\langle \eta^2 \rangle}\mathcal{J}} \tag{33}$$

where

$$\mathcal{J} = 1 - \frac{2\varepsilon_1}{\langle \eta \rangle} \tanh \frac{\langle \eta \rangle}{2\varepsilon_1}$$

and

$<\eta^2> = \eta^2$ evaluated at $C_i = \beta_i$

e. High carrier concentration. The Ward analysis [2] for the limit of high carrier concentration gives

$$\frac{N_1}{N_1^0} = \frac{\sqrt{Y_0}}{2\varepsilon_1} \operatorname{Coth} \frac{\sqrt{Y_0}}{2\varepsilon_1} \tag{34}$$

In the limit $\alpha_1 \to 0$, Eqns 33 and 34 reduce, up to a first approximation, to Eqn 28.

f. Quasilinearization. The numerical solution to the CO_2–HCO_3^- equation, Eqn 26 is obtained by the quasilinearization technique [27, 28]. The quasilinearization procedure was initiated at small diffusion path lengths and a cubic profile for the concentrations assumed:

$$C_i \cong \sum_{j=0}^{3} a_{ij} x^j \qquad i = 1, 3 \tag{35}$$

The constants a_{ij} are evaluated by applying the boundary conditions on C_i: $a_{10} = 1$; $\Sigma_{j=0}^{3} a_{1j} = \rho$; $2a_{12}+3a_{13} = 0$ and $a_{31} = 0$; $2a_{32}+3a_{33} = 0$.

An additional relationship results by virtue of reaction invariant equation, Eqn 27: $a_{32} = -a_{12}/g$

The two unknowns a_{11} (related to the flux of CO_2 at the two boundaries) and a_{20} (the HCO_3^- concentration at $x = 0$) are obtained from the first order near-diffusion regime solution, Eqn 28.

Typical solutions

The various limiting analytical solutions, the boundary layer approximation and the numerical solution outlined above are examined here in order to form a complete picture of the CO_2 facilitation system.

Fig. 1 shows facilitation factor F as a function of the diffusion-reaction parameter α_1 (Damköhler number). Although the analytical solutions in the near-diffusion regime, Curve I, and the near-equilibrium regime, Curve IV, have limited convergence, such solutions nevertheless provide one with an approximate shape of the facilitation curve. The range of validity of the boundary layer approximation, Curve V, far exceeds the range in which either of the other asymptotic solutions are valid. At higher values of the diffusion-reaction resistance, α_1, the numerical solution begins to break down, due principally to extreme concentration gradients near the boundary $x = 1$ [28]. It is in this region of Damköhler number α_1, where the quasilinearization numerical analysis nor the asymptotic solutions are valid, that the boundary layer approximation has maximum utility. Even in regions where the numerical method gives a correct solution, the boundary layer approximation is preferred due to its low computational cost. The latter method tends to break down at exceedingly low Damköhler numbers; failure was evident as the computations did not converge (oscillated between two limits) or negative facilitations were calculated*.

The calculated CO_2, N_1, flux at various values of diffusion path lengths L is shown in Fig. 2. Also included in Fig. 2 are fluxes of CO_2 across a (i) water film, N_1^{ω}; (ii)

* See Notes added in Proof (A), p. 439

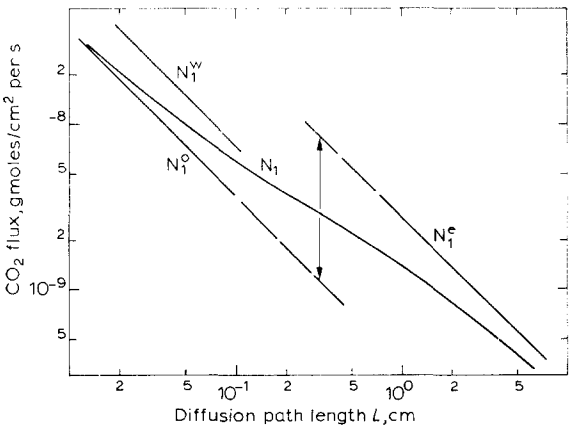

Fig. 2. Expected total CO_2 flux across a membrane (of thickness L) containing 1 M $NaHCO_3$. Calculations are for CO_2 partial pressures at the two boundaries of 1.0 and 0.01 atmos.

1 M $NaHCO_3$–Na_2CO_3 film in absence of any reaction, $N_1{}^o$; (iii) 1 M $NaHCO_3$–Na_2CO_3 film at chemical reaction equilibrium, $N_1{}^e$ **.

EXPERIMENTAL METHODS

The experimental equipment used in this study is essentially the same as the one described by Wittenberg [29] and used by Bassett and Schultz [30]. Only a brief description of the equipment is presented here. Relevant membrane properties and the enzyme activity estimates are also included in this section.

Experimental equipment

The experimental equipment consists of the following components: (a) Gas cylinders containing CO_2, N_2, and He. N_2 was used to obtain the desired partial pressure of CO_2 in the upstream chamber of the diffusion cell. He was used as the carrier gas in the gas chromatograph as well as to sweep away the CO_2 (and N_2) that diffused across the test membrane. (b) A gas saturator made of spargers placed in water-filled flasks to humidify all gases prior to their entry into the diffusion chambers. This step was necessary in order to avoid loss of water from the test membrane due to evaporation. (c) A lucite diffusion cell made up of two chambers, which will be referred to hereafter as the upstream and downstream chambers. A membrane consisting of a microporous filter saturated with the test solutions was interposed between the two chambers, and gas mixtures of known composition were circulated through the upstream and downstream sides. The circular area of the membrane exposed in the diffusion cell was 15.5 cm^2. The diffusion cell and gas humidifier flasks were placed in a water bath maintained at 25±0.5 °C. (d) Soap bubble flow meter (volume: 10 cm^3) placed at the exit of downstream chamber of the diffusion cell to measure accurately the flow rate of the downstream gas mixture. The CO_2 flux was calculated from the total flow rate and composition of the downstream gas mixture. (e) A water vapor trap, consisting of a cooling finger placed in an ice–H_2SO_4 flask for removing

** See Notes added in proof (B), p. 439

water to protect the silica gel column packing in the gas chromatograph. (f) A gas chromatograph and accessories (thermal conductivity cell, recorder, and integrator) for analysis of dried influent and effluent gas samples. The gas chromatograph was equipped with a silica gel column (diameter: 1/8 inch, length: 6 feet) to facilitate separation of CO_2 and N_2. The pressure drop between the diffusion chamber and the gas chromatograph was approximately two inches of water. For all purposes, the partial pressure indicated by the gas chromatograph is assumed to be that at the exit of the diffusion chamber. In each of the diffusion chambers, the gas is assumed to be well mixed*.

Appropriate downstream partial pressure of CO_2 was obtained by adjusting the flow rate of He through the downstream chamber of the diffusion cell**. Various diffusion path lengths were obtained as a "sandwich" formed by placing two or more Gelman membranes side-by-side.

Membrane properties

A highly porous Gelman GA-6 membrane*** with the following nominal specifications was used to support the liquid film used in this study: thickness, 150 μm; mean pore size, 0.45 μm; porosity, 85 %.

The properties of the Gelman membrane that are of interest to this study are the membrane thickness, porosity, and tortuosity. The thickness and porosity of the membrane were calculated from volume estimates. The "dry" volume of the membrane was estimated from the weight of a sample (membrane polymer density: 1.66 gm/cm^3). Subsequently, the sample was soaked in distilled water, and the volume of water estimated. The thickness was calculated from total volume per unit area of the sample, and the porosity calculated as the void fraction volume (that is, volume of water/total volume). For a single membrane, the volume measurements gave the following average results: thickness, 162.3 ± 10.8 μm; porosity, 0.883 ± 0.013.
Measurements on a sandwich of 3–5 membranes revealed that negligible inter-membrane liquid was present.

The diffusion thickness of each membrane is greater than the geometrical thickness because of tortuosity. Based on measurements of CO_2 diffusion through membranes containing only water and no carbonates, a membrane tortuosity of 1.21 was estimated [7] and therefore a diffusion thickness of 200 μm per membrane was used.

Enzyme assay

The activity of enzyme carbonic anhydrase was studied by following the enzyme hydrolysis of *p*-nitrophenyl acetate. Acetazolamide, an inhibitor that binds 1:1 with the enzyme, was used at a number of different levels to titrate the amount of active enzyme available for hydrolysis [31]. From these kinetic studies, the activity of a 1 mg/ml enzyme solution was estimated to be 88 % and it decreased to roughly 77 % at the end of one year. For purposes of subsequent calculations, an enzyme activity of 80 % will be assumed.

---

* The volumetric flow rate of gases through the diffusion chambers ranged from 20 to 80 cm^3/min.

** Gelman Instruments Company, Ann Arbor, Mich.

*** It was not possible to obtain the same values of P_L in all experiments; in most cases P_L/P_0 was less than 0.04.

Certain precautions were necessary in handling of enzyme carbonic anhydrase. The enzyme solution was prepared at a concentration of 1 mg/ml and stored in 2-ml portions at −40 °C. The solid enzyme sample was stored at 4 °C. 1 day prior to the experiment, the enzyme solution was removed and placed in water maintained at 4 °C.

RESULTS

The presence of dissolved Na_2CO_3 and $NaHCO_3$ within the film has two competing effects: namely, a decrease in the CO_2 flux due to decreased solubility and diffusivity of CO_2, and an increase in the CO_2 flux due to the reaction-related facilitation effect. The aim of this section is to investigate the latter effect in detail.

Facilitation in the flux of CO_2-uncatalyzed reaction

The results of experiments at three different path lengths, and at various partial pressure driving forces, are shown in Fig. 3. The total sodium base concentration

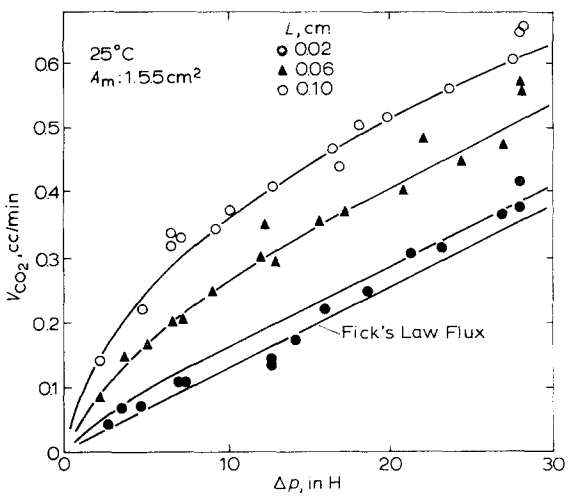

Fig. 3. Experimental and calculated flux of CO_2 at various CO_2 partial pressures. (Ordinate represents flux at $L = 0.02$ cm. At $L = 0.06$, 0.10 cm, ordinated scaled to give identical Fick's law flux), i.e. measured V_{co_2} multiplied by 3 and 5 respectively). Calculations made by boundary layer approximations method, see appendix II.

($\hat{C}_6{}^0$) in all these experiments was 1 gmole/l. Also shown in Fig. 3 is the expected unfacilitated Fick's Law flux of CO_2 across the film based on a CO_2 permeability D_1H_1 of $3.80 \cdot 10^{-10}$ mole $\cdot$ cm$^{-1} \cdot$ atm$^{-1} \cdot$ s^{-1} determined by an extrapolation procedure given in a separate study [7]. The facilitation factors F at diffusion path lengths of 600 μm and 1000 μm are shown in Fig. 4. As should be expected, the facilitation factor is observed to increase monotonically with increasing diffusion path length. That the uncatalyzed reaction is far from equilibrium is seen by comparing the corresponding maximum equilibrium facilitation factors (i.e. for $\alpha_1 \to \infty$) which range from 5.6 to approx. 80 for this same range of conditions.

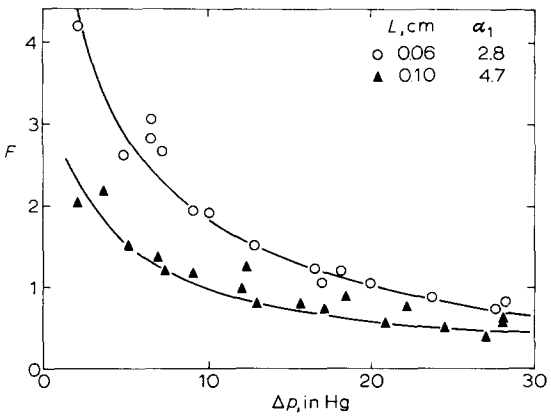

Fig. 4. Facilitation factor at various CO_2 partial pressures and thicknesses across 1 M $NaHCO_3$ membrane. Data of Fig. 3 recalculated.

Facilitation in the flux of CO_2–enzyme-catalyzed reactions

In order to investigate the near-equilibrium regime for this system, it is necessary to increase the Damköhler number to 100 or more. This was achieved by the introduction of carbonic anhydrase which catalyzes the hydration reaction.

The flux of CO_2 at a diffusional path length of 200 μm and an enzyme concentration of 0.08 mg/ml (based on 80 % activity of enzyme preparation) is shown in Fig. 5 at various partial pressure driving forces. The experiments were conducted over a period of 8–12 h and on three different occasions. For each of the three runs, a fresh $NaHCO_3$ solution was prepared and a new carbonic anhydrase sample used. The enzyme is seen to produce a very significant effect on the CO_2 flux; at a partial pressure driving force of about 0.1 atmos., the CO_2 flux is at least 10-fold higher than that observed in the absence of the catalyst. The lower solid straight line in Fig. 5 is the estimated CO_2 flux in absence of any facilitation reactions. The solid curve adjacent to the data points, in this and subsequent figures represents the solution to the

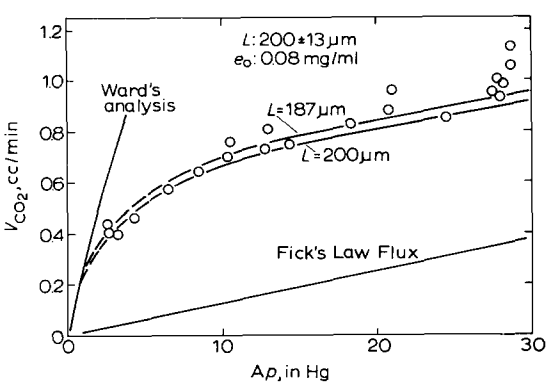

Fig. 5. Flux of CO_2 across a 0.02-cm membrane containing 1 M $NaHCO_3$ and 0.08 mg/ml carbonic anhydrase.

enzyme-catalyzed diffusion reaction equations, Eqn 27, by the boundary layer approximation (see Appendix II).

In the limit of zero partial pressure driving force, the approximate method of Ward [2] is of great use, for it provides the limiting slope of the CO_2 flux at zero partial pressures. An interesting observation is that as the limit of zero concentration of the transferred species is approached, the carrier, normally a mediator in the transport of CO_2, becomes the principal transport mode for CO_2. The expected concentration profiles in this limit will be presented below.

The next series of experiments were designed to investigate the relationship between the diffusion path length and enzyme concentration (or reaction rate constant). As indicated earlier in Eqn 27, for the enzyme-catalyzed reaction of CO_2 the diffusion–reaction resistance and the kinetic function expressions were

$$\alpha_e^2 = \frac{k_p E_0}{K_{ms}} \frac{L^2}{D_1}, \qquad \phi_e = \left(\tilde{C}_1 - m \frac{C_3^2}{1 - C_3}\right) / Q$$

The facilitation factor, F, depends, among other factors, on α_e, therefore on the enzyme concentration E_0 and diffusion length L. But since E_0 and L do not appear elsewhere in the equations, it would be expected that if the product E_0L^2 is maintained constant, the facilitation factor F should also be a constant even if the individual values of enzyme concentration and thickness are changed. The results of the experiments at two different path lengths and enzyme concentrations, but a constant value of E_0L^2, are shown in Fig. 6. The solid lines adjacent to the experimental data are calculated fluxes at two different downstream partial pressures, P_L; the latter ranged from $5 \cdot 10^{-3}$–$1.17 \cdot 10^{-2}$ atmos. in the experiments. The facilitation factor F for these experiments is plotted in Fig. 7. It is noted that an increase in α_e (due either to increased L or E_0) results in an increased facilitation factor F. The results also indicate that the constancy of E_0L^2 does indeed result in the same measured facilitation factor.

Otto [21] observed that in the presence of 1 M $NaHCO_3$, the enzyme-catalyzed CO_2 reaction rate did not increase in direct proportion to the total enzyme concentration, E_0. If this is the case, then the kinetic function, ϕ_e, would also contain terms in

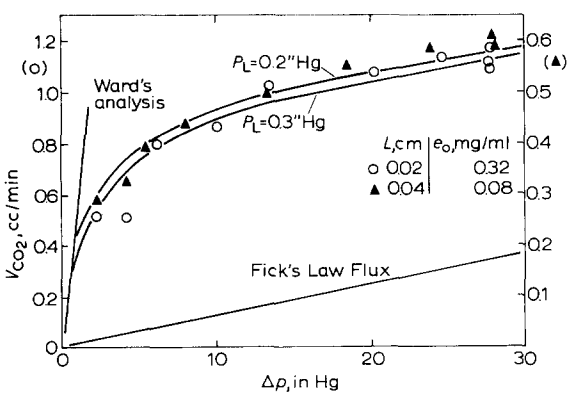

Fig. 6. Flux of CO_2 at a fixed Damköhler number (constant E_0L^2) illustrating that the reaction rate increases linearly with enzyme concentration. Note different scales used to compensate for greater Fick's Law flux obtained with thinner membranes.

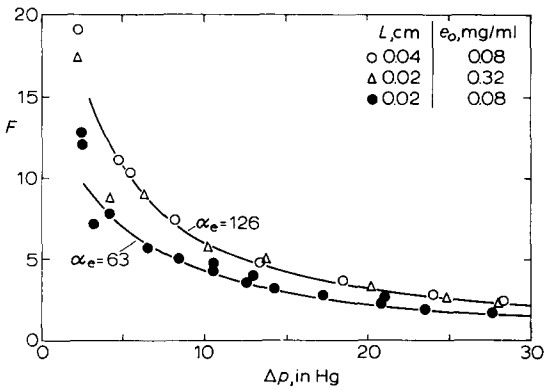

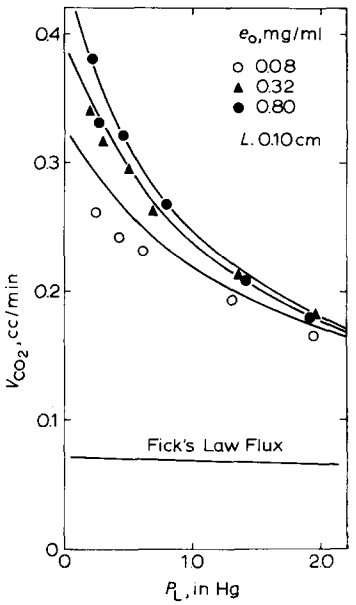

Fig. 7. Facilitation factor at various CO_2 partial pressures and thicknesses across a 1 M $NaHCO_3$ membrane containing carbonic anhydrase.

Fig. 8. Flux of CO_2 across a 0.10-cm membrane containing 1 M $NaHCO_3$ and carbonic anhydrase as a function of downstream (back) partial pressure of CO_2.

enzyme concentration, E_0, and mere constancy of E_0L^2 would not be sufficient to obtain a unique value of facilitation factor F. The fact that our experimental results conform to such a unique relationship leaves the discrepancy between Otto's results and ours still to be explained.

The relationship between the diffusion–reaction resistance, α_e, and downstream CO_2 partial pressures was investigated further. The results reported in Fig. 8 are for a diffusional path length of 0.1 cm. (corresponding to a composite of five Gelman membranes) and at three carbonic anhydrase concentrations. At lower downstream CO_2 partial pressures, increasing enzyme concentration (or, in other words, α_e) resulted in a corresponding increase in the CO_2 flux. Such an observation would indicate that the condition of chemical reaction equilibrium has not yet been attained. On the other hand, at higher downstream CO_2 partial pressures, the observed increase in flux at higher enzyme concentrations is comparatively small, indicating that chemical reaction equilibrium exists in most parts of the film. The drop in CO_2 flux due to an increased downstream CO^2 partial pressure P_L is extremely significant; at an enzyme concentration of 0.8 mg/ml, changing P_L from 0.0066–0.066 atmos., a 6% difference in the overall gradient, results in a reduction of the CO_2 flux from 0.38 to 0.18 cm^3/min.

DISCUSSION

In the uncatalyzed facilitation experiments several interesting features emerge from the fact that the system is in the near-diffusion regime as indicated by the rather

small observed facilitation factors. First, the downstream CO_2 partial pressure, P_L, has negligible effect on the facilitation factor. Secondly, in this regime, calculations of facilitation show that fluxes are relatively insensitive to a number of parameters that affect it. For example, recall that the first-order near-diffusion solution, Eqn 28, did not contain any terms in carrier diffusivity. As a consequence, for the model solution indicated in Fig. 3 and 4, the facilitation factor changed by less than 2 % for a carrier diffusivity change of over 20 %. The diffusion–reaction resistance parameter α_1 at a path length of 1000 μm is roughly 5.

Although one has exceeded the convergence limit of the near-diffusion regime analysis, the carrier diffusivity effect is nevertheless small. Yet another factor, the diffusivity of CO_2, affects the model solution only slightly in this regime – a 20 % change in diffusivity resulting in a change in the facilitation factor by less than 1 %.

The model solution indicated in Figs 3 and 4 are for the following parameter values:

k_1	$0.0375\ s^{-1}$
K'	0.105 gmole $\cdot$ cm^{-3} $\cdot$ atm^{-1}
n	11.46
D_1H_1	$3.80 \cdot 10^{-10}$ moles $\cdot$ cm^{-1} $\cdot$ atm^{-1} $\cdot$ s^{-1}
D_1	$1.6 \cdot 10^{-5} \pm 0.2 \cdot 10^{-5}$ cm^2/s
D_3	$0.88 \cdot 10^{-5} \pm 0.1 \cdot 10^{-5}$ cm^2/s
ρ	0.01–0.04

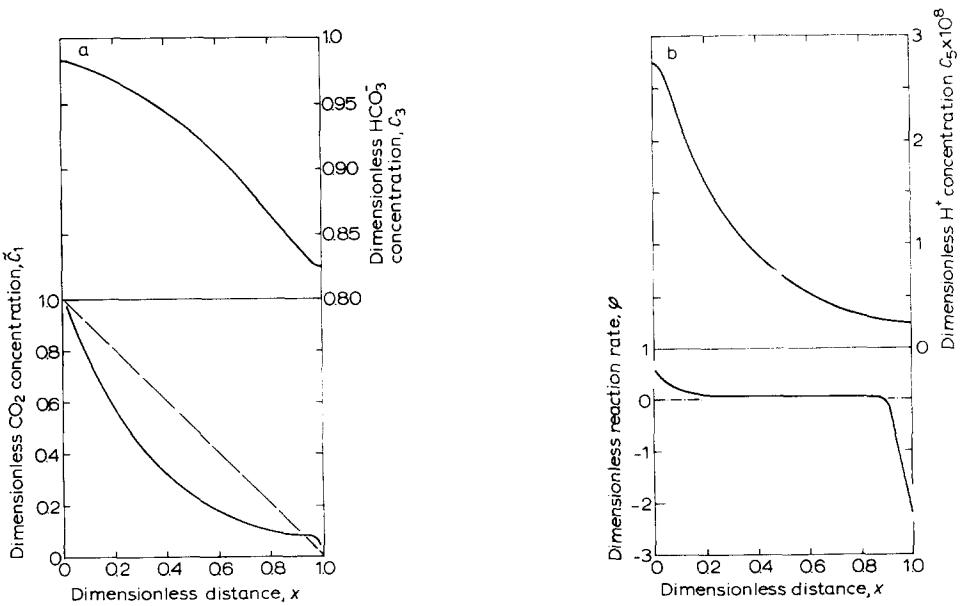

Fig. 9. Dimensionless concentration (CO_2, HCO_3^-, H^+) and reaction (ϕ) profiles within a membrane. Thickness L, 0.5 cm; P_0, 1.0 atmos.; ρ, 0.01.

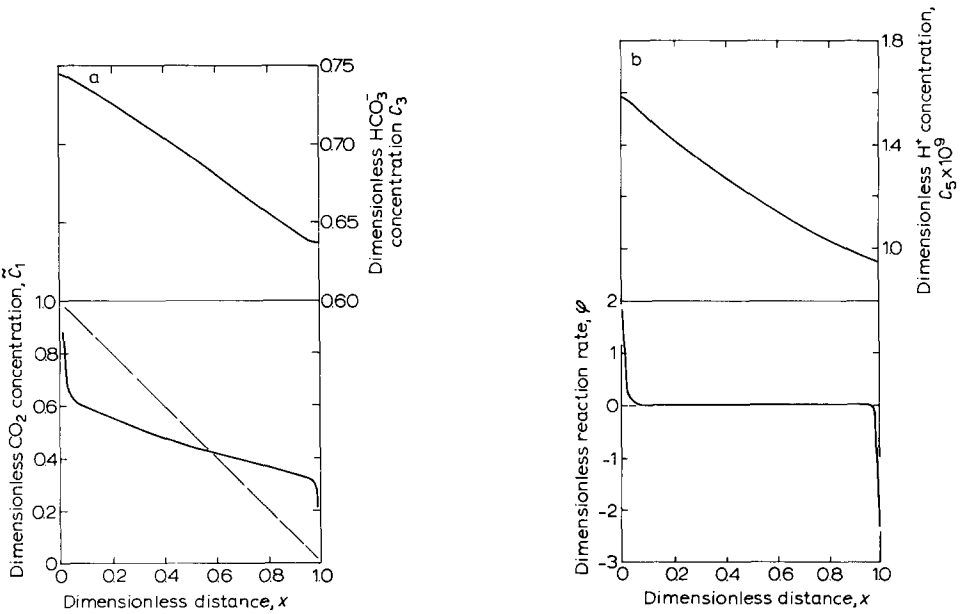

Fig. 10. Dimensionless concentration (CO_2, HCO_3^-, H^+) and reaction (ϕ) profiles within a membrane. Thickness L, 0.5 cm; P_0, in Hg; ρ, 0.01.

The calculated concentrations of CO_2 ($\tilde{C}_1$), HCO_3^- (C_3), and H^+ (C_5), and the reaction rate within the film at an imposed CO_2 partial pressure, P_0, of 1.0 atmos. and 0.066 atmos. are shown in Figs 9 and 10, respectively. The calculations are for a film thickness of 0.5 cm, corresponding to $\alpha_1 = 23.4$. Several theoretical features of CO_2–HCO_3^- facilitated transport phenomenon are evident, namely: (a) The reaction boundary layer phenomenon of Goddard et al. [8] is highly visible, as evidenced by finite reaction rates in the regions close to the boundaries. (b) At the lower P_0, the transport process inside the core region approaches a form of strictly carrier transport; the latter being defined as a transport process wherein the carrier is the sole mediator of transport process. (c) The Ward analysis [2] for the limit of "large carrier concentration" gives, at an upstream CO_2 partial pressure $P_0 = 0.066$ atmos. a facilitation factor, F, twice as large as one calculated here although $<\hat{C}_3> \cong 800$ $<\hat{C}_1>$. As such, for this particular case, one concludes that the "large carrier concentration" limit has not yet been achieved. (d) The pH across the film varies by 0.3 unit at the lower P_0 and 1.0 unit at the higher P_0; the minimum and maximum pH within the film being 7.56 and 9.08. The assumption regarding negligible H^+ and OH^- concentration within the film made earlier in simplifying the model equations is therefore valid.

Inasmuch as the errors and deviation in the experimental data ($\pm 4\%$) are significantly higher than the sensitivity of the model solution to its parameters, one cannot use the experimental data in the near diffusion regime to obtain accurate values of certain parameters, such as CO_2 and carrier diffusivities.

In the enzyme-catalyzed facilitation experiments, the solid lines adjacent to the data points represent solution to the model, Eqn 27. The model parameters were

chosen with a view of obtaining a best fit between model solution and experimental results for all the enzyme facilitation data reported in this study. A set of model parameters which resulted in an excellent agreement between model solution and experimental results for a given set of data did not necessarily result in similar agreement for a different set of data. The set of model parameter listed in Table II resulted in a model solution which agreed with all the experimental data to within $\pm 10\,\%$.

TABLE II

Parameter	Parameter value "Best Fit"	Literature
k_p^0, s^{-1}	$8 \cdot 10^5$	$8 \cdot 10^5$ [13]
K_{ms}, gmoles/cm^3	$12 \cdot 10^{-5}$	$12 \cdot 10^{-5}$ [13]
K_H, gmoles/cm^3	$5 \cdot 10^{-12} \pm 1 \cdot 10^{-12}$	$4.6 \cdot 10^{-13}$ [13]
K_{mi}, gmoles/cm^3 $Q = Q_1$	$1 \cdot 10^{-3} \pm 0.2 \cdot 10^{-3}$	
$Q = Q_2$		
K', gmoles $\cdot$ cm^{-3} $\cdot$ atm^{-1}	0.12 ± 0.1	0.105
D_3, cm^2/s	$0.80 \cdot 10^{-5} \pm 0.01 \cdot 10^{-5}$	$0.89 \cdot 10^{-5}$★
D_1H_1, gmoles $\cdot$ cm^{-1} $\cdot$ atm^{-1} $\cdot$ s^{-1}	$3.8 \cdot 10^{-10} \pm 0.1 \cdot 10^{-10}$ [7]	
D_1, cm^2/s	$1.6 \cdot 10^{-5} \pm 0.1 \cdot 10^{-5}$	

★ Estimated in Psysicochemical parameters.

For the data presented, the model solutions based on the kinetic mechanisms of Kernohan [13] and Haldane [26] cannot be distinguished. The ionization pH of the enzyme carbonic anhydrase appears to be about 1 unit less than that reported by Kernohan [13]. A significant conclusion of this study seems to be that the facilitation experiments presented here may not be used either to investigate the kinetic mechanism of a reaction scheme or to determine, with any degree of accuracy, certain model parameters. A non-linear regression analysis of the flux data would be of little use in obtaining accurate model parameter value since only a significant change in the model parameters will show any change in the calculated flux. For example, the HCO_3^- diffusivity has to be changed by at least ten percent to obtain a 2 %, or so, change in the calculated flux. The errors in measured flux being of the order of $\pm 4\,\%$, no accurate information regarding the bicarbonate diffusivity can be obtained. Suffice it to say that for the model described here, a reasonable fit is obtained between the model solution and the experimental results.

A final comment regarding some observations by Otto and Quinn [6] is in order. At a diffusion path length of 630 μm and a K^+ concentration of 1 and 2 M, Otto and Quinn report that the ratio of the observed flux to the calculated equilibrium flux reaches a maximum at an enzyme concentration of 0.5 mg/ml; at higher enzyme concentrations, the said ratio levels out. This behavior is contrary to the predictions of the diffusion–reaction equations used in this study. Otto and Quinn attribute their observation to some abnormal enzyme phenomena, such as changes in the enzyme orientation at high concentrations. Their results on inhibition of the enzyme by HCO_3^- indicate that the rate of reaction of CO_2 in enzyme solutions increases monotonically, though not linearly, with the enzyme concentration. As a result, the facili-

tation in the flux of CO_2 should also increase monotonically with increasing enzyme concentration. The results reported here indicate that the flux of CO_2 at a given set of parameter values such as film thickness, upstream and downstream CO_2 partial pressure always increased with increasing enzyme concentration.

In terms of the separation of permeable substances across membranes, it should be noted that whereas the facilitation factor, F, (and therefore the extent of separation of gases) increases at high diffusion path lengths (or Damköhler numbers) and lower interfacial concentrations, the corresponding value of the absolute CO_2 flux decreases. An optimum condition is therefore obtained when the facilitation factor, F, as well as the CO_2 flux are high. For the system studied here one such optimum condition appears to be at a diffusion path length of 200 μm or less, CO_2 partial pressure, of about 1/6 atmos. at the gas–liquid interface, and the presence of $NaHCO_3$ (1 M) and enzyme carbonic anhydrase (0.5 mg/ml or more). The CO_2 flux under these conditions would be roughly $3 \cdot 10^{-8}$ gmole $\cdot$ cm$^{-2} \cdot$ s^{-1}; the flux of O_2 under identical conditions is roughly $1.2 \cdot 10^{-10}$ gmoles $\cdot$ cm$^{-2} \cdot$ s^{-1}, giving a CO_2/O_2 separation factor of about 250. Alternatively, if air at one atmosphere (CO_2: 0.033 %) was maintained at the gas–liquid interface, the ratio of CO_2 flux to the N_2–O_2 flux would be about 1 compared to only 1/60 across a corresponding water film.

SUMMARY AND CONCLUSIONS

HCO_3^- and CO_3^{2-} entrapped within a liquid film were found to facilitate, or enhance, the flux of carbon dioxide across the liquid film as a result of the following reversible reaction within the film: $CO_2 + CO_3^{2-} + H_2O \rightleftarrows 2HCO_3^-$. The facilitation studies were carried out in a $NaHCO_3$ solution; the reaction scheme then involves a total of nine species and six kinetic steps. An analysis based on assuming the validity of the macroscopic diffusion and kinetic equations at every point within the film and the following further conditions accounted for all aspects of the experimental data: (a) Electrical effects are absent and the membrane is electrically neutral, (b) diffusion process may be described by binary diffusivities and mobility interactions are absent, (c) at the liquid–gas interface, the partial pressure in the gas phase is related to the concentration in the liquid phase via a Henry's law constant. Of the six kinetic steps, only the two involving CO_2 are rate limiting; the remaining four being extremely rapid and therefore assumed to be at chemical equilibrium. The mathematical treatment of the diffusion–reaction equations were simplified on the basis of the observations that (a) $D_{HCO_3^-} \cong D_{CO_3^{2-}}$; (b) $H^+ \ll Na^+$; (c) $OH^- \ll HCO_3^- + 2CO_3^{2-}$, (d) $NaHCO_3$ fully dissociated.

Enzyme carbonic anhydrase was used as a catalyst in the CO_2 reactions. In analyzing the enzyme catalyzed reactions it was assumed that the rate of CO_2 conversion was directly proportional to the total enzyme concentration.

The solutions to the mathematical model indicate that with increasing Damköhler number the extent of facilitation increases monotonically and approaches the limit of equilibrium facilitation. The experimental study conformed to such a prediction and no abnormal behaviour in the kinetics of enzyme carbonic anhydrase were noticed.

Two different kinetic inhibition schemes for the enzyme catalyzed reactions

gave numerical results that were almost identical (within $\pm 2\%$). In light of this, reasonable correspondence between model calculations and experimental data should be viewed with some caution as evidence for a particular model. Also, precise information regarding model parameter values and/or the determination of a reaction kinetic scheme should not be expected from such an experimental arrangement.

In considering the physiological significance of this study, one must allow for a number of differences in the physiological transfer of CO_2. The diffusion path length of a biological cell being considerably smaller than thicknesses studied here, the enzyme carbonic anhydrase would play a major role in the transfer of CO_2. The physiological reaction medium contains, besides the HCO_3^- ion, several other species, such as HPO_4^{2-} and Cl^- which influence the reactions and catalysis. A direct application of the experimental results presented here to the estimation of CO_2 flux under physio logical conditions without accounting for the differences in composition may be erroneous. However, the mathematical treatment presented here should be of great use in such a context.

APPENDIX I

Justification of simplifications of model equations

All calculations shown below are for a 1 M $NaHCO_3$–Na_2CO_3 solution, that is, $\hat{C}_6^0 = 1$ gmole/l.

(i) In conducting the facilitation studies, a strong dissociating salt (for example, $NaHCO_3$) is added to obtain significant HCO_3^- concentration. Thus, one may safely assume that $K_5 \cong \infty$ or that $C_6 \ll C_4$. Eqn 24a thus simplifies to

$$C_4 \cong 1, \quad \text{at all } x \text{ values} \tag{I.1}$$

(ii) Typical ranges of CO_3^{2-} and HCO_3^- concentration (C_2 and C_3) are: C_2, 0.98^+–0.20; C_3, 0.01–0.40. The ranges of OH^- and H^+ concentration (C_7 and C_5) are calculated from Eqn 22 to be: C_7, $1.1 \cdot 10^{-4}$–$5 \cdot 10^{-7}$; C_5, $1.4 \cdot 10^{-10}$–$3 \cdot 10^{-8}$. In view of this, one may neglect the concentration of OH^- and H^+ from the zero charge density constraint, Eqn 25b, to give

$$\int_0^1 (2C_2 + C_3)\mathrm{d}x \cong \int_0^1 C_4\,\mathrm{d}x \cong 1$$

Further, since it has been shown in a preceding section that $D_2 \cong D_3$ the above constraint reduces to

$$2C_2 + C_3 \cong 1, \quad \text{at all } x \text{ values} \tag{I.2}$$

(iii) Finally, the flux equation, Eqn 26, may be simplified since (a) $D_6 C_6 \cong 0$, at all x values and (b) $C_9 \leqq 10^{-2} C_1$.

Thus,

$$D_1 C_1 + D_2 C_2 + D_3 C_3 \cong p_{13} x + q_{13} \tag{I.3}$$

A further transformation of the diffusion-reaction equations is made so as to relate the CO_2 flux to its partial pressure; thus, Eqn 23 along with the simplifications proposed here is written as

$$\frac{d^2\tilde{C}_1}{dx^2} = \frac{k_1 L^2}{D_1}\phi$$

$$\tilde{C}_1 + gC_3 = p_{13}x + q_{13} \tag{I.4}$$

where

$$\tilde{C}_1 = \hat{C}_1/\hat{C}_1(0)$$

$$\phi = \left(\tilde{C}_1 - \frac{C_3^2}{1-C_3}\right)\left(1 + n\frac{1-C_3}{C_3}\right)$$

$$g = \frac{1}{2}\frac{D_3\hat{C}_6^0}{(D_1 H_1)P_0}$$

$$m = \frac{2\hat{C}_6^0}{(KH_1)P_0} \qquad n = \frac{k_2 K_6}{2k_1 K_4}$$

The boundary conditions on Eqn I.4 are

$$\tilde{C}_1(0) = 1$$

$$\tilde{C}_1(1) = \rho \equiv P_L P/_0 \tag{I.5}$$

$$\frac{dC_3}{dx} = 0 \quad \text{at} \quad x = 0, 1.$$

APPENDIX II

Boundary layer approximation

Kreuzer and Hoofd [9, 32] and Smith et al. [10] have presented a boundary layer approximation for solving the non-linear diffusion–reaction equations. The approximation presented by these authors was limited to reactions of the type: $A_1 + A_2 \rightleftarrows A_3$. Their approach is generalized herein so as to be applicable to any arbitrary kinetic function ϕ.

The governing equations for facilitated transport phenomenon in the presence of single chemical reaction may be written as

$$\frac{d^2C_i}{dx^2} = g_i\alpha^2\phi \tag{II.1}$$

$$g_i C_j - g_j C_i = p_{ij}x + q_{ij} \tag{II.2}$$

$$\int_0^1 (\text{Carrier})dx = C_3^0 \tag{II.3}$$

where $g_i = D^\star/D_i\nu_i$, $\alpha^2 = k^\star L^2/D^\star$, $\phi = \omega/k^\star C^\star$, $C_i = \hat{C}_i/C^\star$ and $x = y/L$.
It can be shown that, for any set of given p_{ij} and q_{ij}, there exist concentration functions ψ_i which satisfy the equilibrium relationship and the stoichiometric invariance relationships:

$$(\phi)_{\psi_i} = 0 \tag{II.4}$$

$$g_i\psi_j - g_j\psi_i = p_{ij}x + q_{ij} \tag{II.5}$$

The perturbation of the "actual" concentration functions C_i from the equilibrium concentration functions ψ_i may be defined by a single parameter:

$$C_i = \psi_i + g_i \delta \tag{II.6}$$

The parameter δ behaves in a manner similar to the boundary layer correction of Goddard et al. [8]. Within the central portion of the film, the equilibrium concentration functions adequately describe the transport process and $\delta \to 0$. Within regions close to the boundaries, δ permits one to correct for deviations from equilibrium; however, such deviation may not necessarily be a result of finite α alone.

The kinetic function ϕ is now expanded in a (first-order) Taylor series around the equilibrium concentration functions; thus,

$$\phi = \Phi + \eta^2 \delta \tag{II.7}$$

where $\Phi \equiv (\phi)_{\psi_i} = 0$, $\eta^2 = \Sigma_j \phi^j g_j$ and $\phi^j = \partial\phi/\partial C_j$ at $C_j = \psi_j$.
Substituting the concentration and kinetic functions, Eqns II.6 and II.7, into the diffusion–reaction equation, Eqn II.1, gives:

$$\frac{d^2\psi_i}{dx^2} + g_i \frac{d^2\delta}{dx^2} = g_i \alpha^2 \eta^2 \delta \tag{II.8}$$

Since the parameter δ need be evaluated only in the "boundary" layer regions, Eqn II.8 is solved in regions close to the boundaries, that is, near $x = 0$ and $x = 1$. Within these regions it may be shown [9]

$$\left| \frac{d^2\psi_i}{dx^2} \right| \ll \left| \frac{d^2\delta}{dx^2} \right|$$

and that the kinetic function derivatives ϕ^j are constants, obtained by evaluation at the boundaries; thus,

$$\text{Near } x = 0, \quad \frac{d^2\delta}{dx^2} = \bar{\eta}^2 \alpha^2 \delta \tag{II.9}$$

$$\text{Near } x = 1, \quad \frac{d^2\delta}{dx^2} = \underline{\eta}^2 \alpha^2 \delta$$

The solution to Eqn II.9 is

$$\text{Near } x = 0 \quad \delta = \bar{\delta} e^{-\bar{\eta}\alpha x}$$

$$\text{Near } x = 1 \quad \delta = \underline{\delta} e^{-\underline{\eta}\alpha(1-x)} \tag{II.10}$$

where the constants $\bar{\delta}$ and $\underline{\delta}$ are the values of δ at $x = 0$, 1, respectively; these are evaluated by using the non-transference boundary condition on carrier species; thus,

$$\psi_3'(0) = g_3 \bar{\delta} \bar{\eta} \alpha$$

$$\psi_3'(1) = -g_3 \underline{\delta} \underline{\eta} \alpha \tag{II.11}$$

The concentration functions for the transferred species, ψ_1 and C_1 at the two boundaries are then given by

$$\bar{C}_1 = \psi_1(0) + \frac{g_1}{g_3}\frac{1}{\bar{\eta}\alpha}\psi_3'(0)$$

$$\underline{C}_1 = \psi_1(1) - \frac{g_1}{g_3}\frac{1}{\underline{\eta}\alpha}\psi_3'(1) \qquad \text{(II.12)}$$

A further simplification may be obtained by utilizing Eqns II.4 and II.5; thus

$$\phi^1\psi_1' + \phi^2\psi_2' + \phi^3\psi_3' = 0 \qquad \text{(II.13)}$$

and

$$g_1\psi_3' - g_3\psi_1' = p_{13}$$
$$g_2\psi_3' - g_3\psi_2' = 0 \qquad \text{(II.14)}$$

Substituting Eqn II.14 into Eqn II.13 and utilizing the definition of η^2 gives

$$\phi^1(g_1\psi_3' - p_{13}) + \phi^2 g_2\psi_3' + \phi^3 g_3\psi_3' = 0$$

or

$$\psi_3' = \frac{\phi^1}{\eta^2}p_{13} \qquad \text{(II.15)}$$

Eqn II.15 in Eqn II.12 gives

$$\bar{C}_1 = \psi_1(0) + \frac{g_1\bar{\phi}^1}{\alpha\bar{\eta}^3}\frac{p_{13}}{g_3}$$

$$\underline{C}_1 = \psi_1(1) - \frac{g_1\underline{\phi}^1}{\alpha\underline{\eta}^3}\frac{p_{13}}{g_3} \qquad \text{(II.16)}$$

Eqn II.6 along with:

$$\Phi = 0$$
$$g_i\psi_j - g_j\psi_i = p_{ij}x + q_{ij} \qquad \text{(II.17)}$$
$$\int_0^1 (\text{Carrier})\mathrm{d}x = C_3^0$$

permits one to calculate, iteratively, the flux factor, p_{13}/g_3.

NOTES ADDED IN PROOF

(A) In the experiments to be described, α_1, the Damkholer number for the uncatalyzed reaction was varied between 1 and 5, and α_e for the enzyme-catalyzed experiments was varied between 30–500.

(B) The decrease in flux in the limit of thin films shown by the difference between $N_1{}^{\omega}$ and $N_1{}^0$, reflects the decreased diffusivity and solubility of CO_2 in 1 M $NaHCO_3$ solution relative to pure water. The actual total "facilitated" flux through the bicarbonate solution, given by N_1, only becomes greater than the CO_2 flux through water when the film thickness exceeds 0.2 cm. In thicker films, the augmenta-

tion due to the CO_2 reaction with carbonate more than compensates for the decreased diffusivity and solubility of CO_2 in these solutions. Note that the total flux always decreases with increasing film thickness, even though the facilitation effect, $N_1 - N_1{}^0$, increases with thickness to the maximum value, $N_1{}^e - N_1{}^0$, shown by the arrow in Fig. 2.

ACKNOWLEDGEMENTS

This work was supported in part by Public Health Service Grant GM15152 and by a Research Career Development Award (Number 1-K4-GM-8271) to Jerome S. Schultz from the Institute of General Medical Sciences.

REFERENCES

1 Danckwerts, P. V. (1970) Gas–Liquid Reactions, McGraw-Hill, New York
2 Ward, W. J. (1967) Report 159384-1, Aerospace Medical Research Labs., Wright-Patterson AF Base, Ohio
3 Ward, W. J. and Robb, W. L. (1967) Science 156, 1481
4 Longmuir, I. S., Foster, R. E. and Woo, C.-Y. (1966) Nature 209, 393
5 Enns, T. (1967) Science 155, 44
6 Otto, N. C. and Quinn, J. A. (1971) Chem. Eng. Sci. 26, 949
7 Suchdeo, S. R. and Schultz, J. S. (1974) Chem. Eng. Sci., in the press
8 Goddard, J. D., Schultz, J. S. and Bassett, R. J. (1970) Chem. Eng. Sci. 25, 665
9 Kreuzer, F. and Hoofd, L. J. C. (1972) Respir. Physiol. 15, 104
10 Smith, K. A., Meldon, J. H. and Colton, C. K. (1973) Am. Inst. Chem. Eng. J. 19, 102
11 Friedlander, S. K. and Keller, K. H. (1965) Chem. Eng. Sci. 20, 121
12 Kern, D. M. (1960) J. Chem. Educ. 37, 14
13 Kernohan, J. C. (1965) Biochim. Biophys. Acta 96, 304
14 Chemical Engineers' Handbook (1963) (Perry, J. H., ed.), McGraw-Hill, New York
15 Siedell, A. and Linke, W. F. (1952) Solubilities of Inorganic and Organic Compounds, 3rd edn Supplement, van Nostrand, New York
16 Harned, H. S. and Owens, B. B. (1958) The Physical Chemistry of Electrolyte Solutions, Reinhold, New York
17 Gibbons, B. H. and Edsall, J. T. (1963) J. Biol. Chem. 238, 3502
18 Ho, C. and Sturtvant, J. M. (1963) J. Biol. Chem. 238, 3499
19 Pinsent, B. R. W., Pearson, L. and Roughton, F. J. W. (1956) Trans. Faraday Soc. 52, 1512
20 Edsall, J. T. and Wyman, J. (1958) Biophysical Chemistry, Vol. I, Ch. 10, Academic Press, New York
21 Näsänen, R. (1946) Acta Chim. Fenn. Suomen. Kemis. 19B, 90 (Chem. Abstr. 41: 5366a)
22 McCoy, H. N. (1903) Am. Chem. J. 29, 437
23 Roberts, D. and Danckwerts, P. V. (1962) Chem. Eng. Sci. 17, 961
24 International Critical Tables (1933) Vol. 5, National Research Council, McGraw-Hill
25 Suchdeo, S. R. (1973) Ph. D. Thesis, University of Michigan
26 Haldane, J. B. S. (1930) Enzymes, Longmans, London
27 Kutchai, H., Jacquez, J. A. and Mather, F. J. (1970) Biophys. J. 10, 38
28 Suchdeo, S. R. and Schultz, J. S. (1971) Chem. Eng. Symp. Series 67 (114), 165
29 Wittenberg, J. B. (1959) Biol. Bull. 117, 402
30 Bassett, R. J. and Schultz, J. S. (1970) Biochim. Biophys. Acta 211, 194
31 Verpoorte, J. A., Mehta, S. and Edsall, J. T. (1967) J. Biol. Chem. 242, 4221
32 Kreuzer, F. and Hoofd, L. J. C. (1970) Respir. Physiol. 8, 208